ISSN 1070-3284, Russian Journal of Coordination Chemistry, 2021, Vol. 47, No. 1, pp. 43–51. © Pleiades Publishing, Ltd., 2021.
Russian Text © The Author(s), 2021, published in Koordinatsionnaya Khimiya, 2021, Vol. 47, No. 1, pp. 48–57.

Heteroleptic Bismuth(III) Dithiocarbamato-Chlorido Complexes of $[Bi(S_2CNR_2)Cl_2]$ and $[Bi(S_2CNR_2)_2Cl]$ ($R = C_3H_7$, *iso*-C_4H_9): Preparation, 1D Polymer Structures, Heteronuclear (^{13}C, ^{15}N) CP MAS NMR, and Thermal Behavior

E. V. Novikova[a], **K. L. Isakovskaya**[b, c], **O. N. Antzutkin**[d, e], **and A. V. Ivanov**[a, *]

[a] *Institute of Geology and Nature Management, Far Eastern Branch, Russian Academy of Sciences, Blagoveshchensk, Russia*
[b] *Nesmeyanov Institute of Organoelement Compounds, Russian Academy of Sciences, Moscow, Russia*
[c] *Mendeleev University of Chemical Technology of Russia, Moscow, Russia*
[d] *Luleå University of Technology, Luleå, Sweden*
[e] *University of Warwick, Coventry, UK*
**e-mail: alexander.v.ivanov@chemist.com*

Received March 18, 2020; revised April 22, 2020; accepted May 6, 2020

Abstract—Crystalline bismuth(III) dithiocarbamato-chlorido complexes $[Bi\{S_2CN(C_3H_7)_2\}Cl_2]$ (**I**) and $[Bi\{S_2CN(iso\text{-}C_4H_9)_2\}_2Cl]$ (**II**) were prepared and comparatively studied by (^{13}C, ^{15}N) CP-MAS NMR spectroscopy, IR spectroscopy, and X-ray diffraction (CIF files CCDC nos. 1971976 and 1971975, respectively). The dithiocarbamate ligands are typically coordinated in the S,S'-*iso*- (**I**) or *aniso*- (**II**) bidentate-terminal mode. In each of the compounds, neighboring molecules are connected through one or two μ_2-Cl^- ligands into zigzag-like polymer chains, in which the central atom has sixfold coordination: $[BiS_2Cl_4]$ (**I**) or $[BiS_4Cl_2]$ (**II**). The binding unit in the polymer chains of **I** is a four-membered $[Bi–(\mu\text{-}Cl)_2–Bi]$ metallocycle in the butterfly conformation (the dihedral angle is 140.51(3)°). Therefore, stronger binding of heteroleptic molecules in polymer chains leads to a considerably shorter interatomic Bi–Bi distances in **I** (4.0904(4) Å) than in **II** (4.8772(4) Å). The thermal behavior of heteroleptic bismuth(III) complexes was studied by simultaneous thermal analysis with recording of TG and DSC curves. Although the major product of thermal transformations of **I** and **II** is Bi_2S_3, the microprobe method also identified the presence of reduced bismuth and $BiCl_3$.

Keywords: bismuth(III) polymer compounds, dialkyldithiocarbamato-chlorido complexes, structural organization, thermal behavior, heteronuclear (^{13}C, ^{15}N) CP-MAS NMR spectroscopy

DOI: 10.1134/S1070328421010036

INTRODUCTION

Along with dithiocarbamate complexes, bismuth(III) also forms dithiocarbamato-halido compounds, which exhibit various mixed coordination spheres [1–8]. Some of these compounds are convenient precursors for one-step thermochemical processes giving nano-sized bismuth(III) sulfide Bi_2S_3 [1]; some other were found to have high cytotoxic activity against cancer cells [2, 3]. Structural data on heteroleptic dithiocarbamato-chlorido compounds of bismuth(III) are rather scarce: currently, the structures have been studied only for four complexes with the composition $[Bi(S_2CNR_2)_2Cl]\cdot L$ ($R = CH_3$ [2], C_3H_7 [4]; $R_2 = C_2H_5$, C_2H_4OH; $L = H_2O$ [5], $R_2 = (CH_2)_4$; $L = CHCl_3$ [1]) and for one binuclear adduct with thiourea $[Bi_2\{SC(NH_2)_2\}_2\{S_2CN(CH_2)_4\}_4(\mu_2\text{-}Cl)_2]$ [6]. However, it is clear that on going from BiX_3 to $[Bi(Dtc)_3]$ (Dtc is the dithiocarbamate ligand), the above complexes should be preceded by compounds $[Bi(Dtc)X_2]$. Indeed, a representative of these bismuth(III) dithiocarbamate halide complexes, $[Bi(S_2CNEt_2)I_2]$, has been prepared and structurally characterized [9]. However, crystallization of the corresponding dichloride analogue from a pyridine solution resulted in the isolation of the adduct $[Bi(S_2CNEt_2)Cl_2(Py)_3]\cdot Py$, which contains both outer- and inner-sphere molecules of the N-donor base [10], while the solvated pentanuclear compound $[Bi_5(S_2CNEt_2)_8Cl_7]\cdot DMF$ was unexpectedly obtained from a dimethylformamide–butanol mixture [11]. Only 13 years later, the crystals of the complexes $[Bi(S_2CNEt_2)X_2]$ (X = Cl, Br) [12] were obtained and studied by X-ray diffraction. Until now, these complexes, together with $[Bi(S_2CNR_2)I_2]$ (R = CH_3 [3], C_2H_5 [9]), are the only representatives of heteroleptic bismuth(III) complexes of this type.

As a continuation of our studies of bismuth(III) complexes, here we report the synthesis and a comparative study of heteroleptic dithiocarbamato-chlorido complexes $[Bi\{S_2CN(C_3H_7)_2\}Cl_2]$ (**I**) and $[Bi\{S_2CN(iso\text{-}C_4H_9)_2\}_2Cl]$ (**II**), which were characterized by the heteronuclear (^{13}C, ^{15}N) CP-MAS NMR spectroscopy. In the 1D polymer structures of the obtained crystalline complexes determined by direct X-ray diffraction method, all chlorine atoms occupy μ_2-bridging positions. By studying the thermal behavior of complexes by simultaneous thermal analysis (STA), we established the course of their thermolysis and identified the intermediate and final products of thermal transformations.

EXPERIMENTAL

Sodium *N*,*N*-dialkyldithiocarbamates $Na\{S_2CN(C_3H_7)_2\}\cdot H_2O$ and $Na\{S_2CN(iso\text{-}C_4H_9)_2\}\cdot 3H_2O$ were prepared by the reaction of dialkylamines, $HN(C_3H_7)_2$ (Merck) and $HN(iso\text{-}C_4H_9)_2$ (Aldrich), respectively, with carbon disulfide (Merck) in an alkaline medium [13].

The synthesis of 1D polymeric complexes of *catena*-poly[di(μ_2-chloro)-(*N*,*N*-dipropyldithiocarbamato-*S*,*S*')bismuth(III)] (**I**) and *catena*-poly[(μ_2-chloro)-bis(*N*,*N*-di-*iso*-butyldithiocarbamato-*S*,*S*')bismuth(III)] (**II**) was prepared by the following reactions:

$$BiCl_3 + Na\{S_2CN(C_3H_7)_2\} = [Bi\{S_2CN(C_3H_7)_2\}Cl_2] + NaCl;$$

$$BiCl_3 + 2Na\{S_2CN(iso\text{-}C_4H_9)_2\} = [Bi\{S_2CN(iso\text{-}C_4H_9)_2\}_2Cl] + 2NaCl.$$

The reactions between $BiCl_3\cdot H_2O$ and $Na\{S_2CN(C_3H_7)_2\}\cdot H_2O$/$Na\{S_2CN(iso\text{-}C_4H_9)_2\}\cdot 3H_2O$ were carried out in acetone solutions. The starting bismuth salts were used in a 3% excess over the stoichiometric amount. The reaction mixtures were magnetically stirred for 1 h and allowed to stand for 24 h at room temperature. Then solutions of the resulting complexes were separated from precipitated NaCl by filtration. Light yellow/bright lemon-yellow crystals of **I**/**II** were prepared by slow evaporation of acetone/acetone–ethanol mixture (1 : 1) at room temperature. The yield was 84.8/82.2%; T_m = 186–190°C/130–134°C.

Compound **I**, IR (KBr; ν, cm^{-1}): 2964 s, 2930 m, 2872 m, 1504 vs, 1463 m, 1430 s, 1380 w, 1364 m, 1343 w, 1305 m, 1271 w, 1243 s, 1190 m, 1146 s, 1102 w, 1086 m, 1039 vw, 1030 w, 959 m, 894 w, 768 w, 750 m, 625 w, 599 w, 530 w; compound **II**, IR (KBr; ν, cm^{-1}): 2965 s, 2948 w, 2930 m, 2919 vw, 2865 m, 1486 vs, 1467 m, 1433 w, 1424 s, 1385 m, 1352 m, 1338 m, 1285 m, 1245 s, 1193 m, 1172 w, 1148 s, 1121 w, 1093 s, 972 m, 918 m, 880 w, 819 w, 615 w, 606 w.

(^{13}C, ^{15}N) CP-MAS NMR (δ, ppm), compound **I**: 189.2 ($-S_2\mathbf{C}N=$); 57.9, 57.6 (1 : 1, $=N\mathbf{C}H_2-$); 22.1, 20.7 (1 : 1, $-\mathbf{C}H_2-$); 13.8, 13.5 (1 : 1, $-\mathbf{C}H_3$); 165.2 ($-S_2C\mathbf{N}=$); compound **II**: 204.3 (25)*, 200.8 (31)* (1 : 1, $-S_2\mathbf{C}N=$); 64.2, 62.4, 59.1, 58.3 (1 : 1 : 1 : 1, $=N\mathbf{C}H_2-$); 29.2, 28.8, 28.2, 28.1 (1 : 1 : 1 : 1, $>\mathbf{C}H-$); 24.5, 23.6, 23.1, 22.9, 22.3, 20.8 (1 : 1 : 1 : 1 : 2 : 2, $-\mathbf{C}H_3$); 142.2, 135.9 (1 : 1, $-S_2C\mathbf{N}=$).

The asterisk marks the asymmetric $^{13}C-^{14}N$ doublets (in Hz) [14, 15].

The (^{13}C, ^{15}N) CP-MAS NMR spectra were measured on an Ascend Aeon (Bruker)[1] spectrometer operating at 100.64/40.55 MHz, with a superconducting magnet (B_0 = 9.4 T), a closed loop of helium condensation through external compressor, and Fourier transformation. Cross-polarization from protons (CP) was used: the $^1H-^{13}C/^1H-^{15}N$ contact time was 2.0/1.5 ms. The $^{13}C-^1H/^{15}N-^1H$ decoupling by a radiofrequency field at the proton resonance frequency (400.21 MHz) was employed [16]. Polycrystalline **I**/**II** samples weighing ~103/63 mg were placed into a 4.0 mm ZrO_2 ceramic rotor. The $^{13}C/^{15}N$ NMR spectra were measured with a magic-angle-spinning (MAS) at the 5300–6300/4000–5000(1) Hz frequency; the number of acquisitions was 720–2000/22700–85880; the proton π/2-pulse duration was 2.7/2.7 μs; the pulse delay was 2.0/2.0 s. The isotropic chemical shifts $\delta(^{13}C)/\delta(^{15}N)$ were referred to one component of the external standard, crystalline adamantane (δ = 38.48 ppm relative to tetramethylsilane)/crystalline NH_4Cl (δ = 0.0 ppm, –341 ppm on an absolute scale [17]) with magnetic field drift correction (frequency equivalent of 0.031/0.011 Hz/h).

The IR spectra of complexes **I** and **II**, pressed into KBr pellets, were measured on an FSM–1201 interference Fourier transform spectrometer in the 400–4000 cm^{-1} range. The instrument was controlled and the spectra were processed using the FSpec program (version 4.0.0.2 for Windows, LLC Monitoring, Russia).

X-ray diffraction study was carried out with plate- (**I**) and column-like (**II**) single crystals on a Bruker Apex II DUO diffractometer at 120 K (CCD detector, MoK_α, λ = 0.71073 Å, graphite monochromator). The structures were solved using the SHELXT program package [18]; the subsequent refinement was carried out by least-squares-method using the OLEX2 program package [19] in the anisotropic approximation

---

[1] Some of the ^{13}C CP-MAS NMR measurements were carried out on a Bruker Avance III 500 spectrometer (Bruker) operating at 125.76 MHz (B_0 = 11.74 T) at the Umeå University, Umeå, Sweden.

Table 1. Crystallographic data, X-ray experiment and structure refinement details for structures **I** and **II**

Parameter	Value	
	I	**II**
Molecular formula	$C_7H_{14}NS_2Cl_2Bi$	$C_{18}H_{36}N_2S_4ClBi$
M	456.21	653.16
System	Orthorhombic	Monoclinic
Space group	$Pna2_1$	$P2_1/c$
Z	4	4
a, Å	7.8651(6)	10.0413(4)
b, Å	16.5286(13)	26.1320(10)
c, Å	10.0539(8)	9.5518(4)
α, deg	90	90
β, deg	90	91.8160(10)
γ, deg	90	90
V, Å^3	1307.00(18)	2505.13(17)
ρ(calcd.), g/cm^3	2.318	1.732
μ, cm^{-1}	141.77	74.85
F(000)	848	1288
Crystal size, mm	0.20 × 0.15 × 0.01	0.66 × 0.20 × 0.18
Data collection range over θ, deg	2.37–29.00	2.03–26.00
Ranges of reflection indices	$-10 \leq h \leq 11$, $-23 \leq k \leq 23$, $-14 \leq l \leq 14$	$-12 \leq h \leq 12$, $-32 \leq k \leq 32$, $-11 \leq l \leq 11$
Number of measured reflections	11470	24550
Number of unique reflections	3460	4924
Number of reflections with $I > 2\sigma(I)$	3035	4292
Number of refined parameters	120	243
R_1 (for reflections with $I > 2\sigma(I)$)	0.0274	0.0254
wR_2 (for all reflections)	0.0578	0.0510
GOOF	0.831	1.067
Residual electron density (min/max), e/Å^3	−1.426/1.285	−1.634/0.577

for non-hydrogen atoms. The positions of hydrogen atoms were calculated geometrically and included in the refinement in the riding model. The key crystallographic data and structure refinement details for **I** and **II** are summarized in Table 1 and selected bond lengths and angles are given in Table 2.

The atom coordinates, bond lengths, bond angles, and temperature parameters for the obtained complexes were deposited with the Cambridge Crystallographic Data Centre (CCDC nos. 1971976 (**I**) and 1971975 (**II**); deposit@ccdc.cam.ac.uk or http://www.ccdc.cam.ac.uk).

The thermal behavior of **I**/**II** was studied by STA with simultaneous recording of thermogravimetry (TG) and differential scanning calorimetry (DSC) curves. The measurements were carried out on an STA 449C Jupiter instrument (NETZSCH) in corundum crucibles covered by lids with a hole for maintaining a pressure of 1 atm during the thermolysis. Heating up to 400°C was performed at a rate of 5°C/min in an argon atmosphere. The sample weight was 4.897–13.235/3.457–10.411 mg. The temperature was measured to an accuracy of ±0.7°C and the weight changes were measured to an accuracy of $\pm 1 \times 10^{-4}$ mg. After thermal analysis of the complexes, the degree of dispersion and morphological details of the residual material were examined on a Zeiss SIGMA scanning electron microscope (Germany) equipped with an Oxford X-MAX electron probe X-ray microanalysis system (UK) with energy and wavelength dispersion. The qualitative determination of the chemical composition was performed by microprobe analysis using an energy-dispersive spectrometer.

Table 2. Bond lengths (*d*, Å), bond angles (ω, deg), and torsion angles (φ, deg) for structures **I** and **II***

Bond	*d*, Å	Bond	*d*, Å
	I		
Bi(1)–S(1)	2.6437(13)	S(1)–C(1)	1.747(5)
Bi(1)–S(2)	2.6323(14)	S(2)–C(1)	1.735(6)
Bi(1)–Cl(1)[a]	2.6823(14)	N(1)–C(1)	1.311(7)
Bi(1)–Cl(2)[a]	2.8798(13)	N(1)–C(2)	1.474(7)
Bi(1)–Cl(1)	3.0668(13)	N(1)–C(5)	1.479(7)
Bi(1)–Cl(2)	2.7717(13)		
	II		
Bi(1)–S(1)	2.7845(10)	S(3)–C(10)	1.731(4)
Bi(1)–S(2)	2.6287(10)	S(4)–C(10)	1.728(4)
Bi(1)–S(3)	2.7590(10)	N(1)–C(1)	1.331(5)
Bi(1)–S(4)	2.6468(10)	N(1)–C(2)	1.480(5)
Bi(1)–Cl(1)	2.9606(10)	N(1)–C(6)	1.476(5)
Bi(1)–Cl(1)[a]	3.0424(9)	N(2)–C(10)	1.332(5)
S(1)–C(1)	1.724(4)	N(2)–C(11)	1.479(5)
S(2)–C(1)	1.740(4)	N(2)–C(15)	1.476(5)
Angle	ω, deg	Angle	ω, deg
	I		
S(2)C(1)S(1)	117.2(3)	S(2)Bi(1)Cl(1)[a]	88.44(4)
S(1)Bi(1)S(2)	68.57(4)	S(2)Bi(1)Cl(2)	88.80(4)
S(1)Bi(1)Cl(1)	70.48(4)	S(2)Bi(1)Cl(2)[a]	85.38(4)
S(1)Bi(1)Cl(1)[a]	95.09(4)	Bi(1)Cl(1)Bi(1)[a]	90.46(4)
S(1)Bi(1)Cl(2)	91.44(4)	Bi(1)Cl(2)Bi(1)[a]	92.71(5)
S(1)Bi(1)Cl(2)[a]	153.94(4)	Cl(1)Bi(1)Cl(1)[a]	109.01(4)
S(2)Bi(1)Cl(1)	136.60(4)	Cl(2)Bi(1)Cl(2)[a]	88.45(3)
	II		
S(1)C(1)S(2)	117.7(2)	S(2)Bi(1)S(4)	85.63(3)
S(1)Bi(1)S(2)	66.33(3)	S(1)Bi(1)Cl(1)	97.00(3)
S(3)C(10)S(4)	118.0(2)	S(2)Bi(1)Cl(1)	160.85(3)
S(3)Bi(1)S(4)	66.48(3)	S(3)Bi(1)Cl(1)[a]	74.21(3)
S(1)Bi(1)S(3)	137.76(3)	S(4)Bi(1)Cl(1)[a]	81.57(3)
S(1)Bi(1)S(4)	78.30(3)	Bi(1)Cl(1)Bi(1)[b]	108.67(3)
S(2)Bi(1)S(3)	87.75(3)	Cl(1)Bi(1)Cl(1)[a]	122.17(3)
Angle	φ, deg	Angle	φ, deg
	I		
Bi(1)S(1)S(2)C(1)	−179.4(4)	S(1)C(1)N(1)C(5)	1.7(7)
S(1)Bi(1)C(1)S(2)	−179.5(3)	S(2)C(1)N(1)C(2)	0.0(7)
S(1)C(1)N(1)C(2)	−178.8(4)	S(2)C(1)N(1)C(5)	−179.5(4)
	II		
Bi(1)S(1)S(2)C(1)	177.7(3)	S(2)C(1)N(1)C(2)	−177.2(3)
Bi(1)S(3)S(4)C(10)	168.8(3)	S(2)C(1)N(1)C(6)	−0.8(5)
S(1)Bi(1)C(1)S(2)	178.0(2)	S(3)C(10)N(2)C(11)	−4.1(5)
S(3)Bi(1)C(10)S(4)	170.3(2)	S(3)C(10)N(2)C(15)	−177.1(3)
S(1)C(1)N(1)C(2)	4.2(5)	S(4)C(10)N(2)C(11)	173.0(3)
S(1)C(1)N(1)C(6)	−179.4(3)	S(4)C(10)N(2)C(15)	0.1(5)

* Symmetry codes: [a] 1/2 + *x*, 1/2 – *y*, *z* (**I**); [a] *x*, 3/2 – *y*, –1/2 + *z*; [b] *x*, 3/2 – *y*, 1/2 + *z* (**II**).

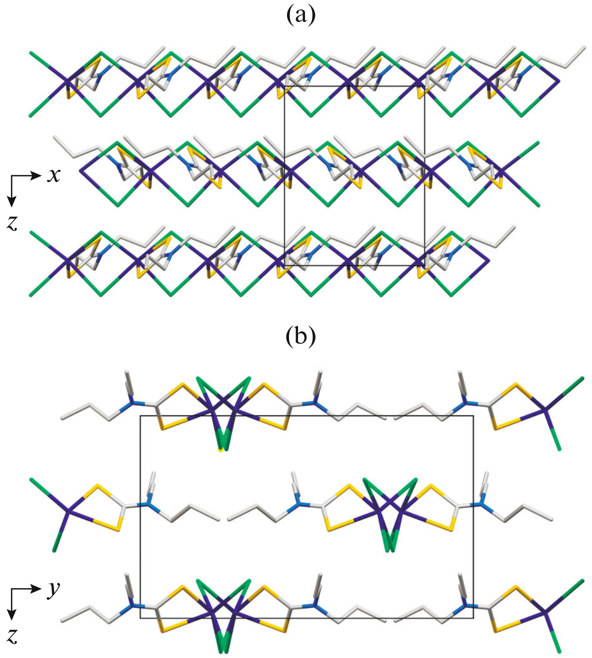

Fig. 1. Projections of the polymer structure of **I** on the (a) *xz* and (b) *yz* planes. The polymer chains are extended along the *x* axis.

RESULTS AND DISCUSSION

In the IR spectra of complexes **I**/**II**, the most intense absorption bands at 1504/1486 cm^{-1} are due to ν(C–N) stretching vibrations of the =NC(S)S– groups of the PrDtc and *iso*-BuDtc ligands. Both values do not fall within the vibration ranges of either ν(C–N) single bonds (1360–1250 cm^{-1}) or ν(C=N) double bonds (1690–1640 cm^{-1}), but occupy an intermediate position between them, which attests to a partially double bond nature of the C$\overset{...}{-}$N bond of the dithiocarbamate groups. In view of the fact that a higher ν(C–N) vibrational frequency corresponds to a greater contribution of double bonding, the shortest N–C(S)S bond among the bismuth(III) dithiocarbamate chloride compounds should be expected for complex **I** (in comparison with **II** or [Bi{S$_2$CN(C$_3$H$_7$)$_2$}$_2$Cl], ν(C–N) = 1493 cm^{-1} [4]). In addition, it is noteworthy that in the series of [Bi{S$_2$CN(C$_3$H$_7$)$_2$}$_3$] (1487, 1476 cm^{-1}) [20], [Bi{S$_2$CN(C$_3$H$_7$)$_2$}$_2$Cl] [4], and [Bi{S$_2$CN(C$_3$H$_7$)$_2$}Cl$_2$], the replacement of the PrDtc ligands by chloride ions is accompanied by a regular increase in the dithiocarbamate C–N vibrational frequency.

The intense absorption bands at 1146/1148 cm^{-1} and the medium-intensity bands at 959/972 cm^{-1} were assigned to asymmetric ν$_{as}$(CS$_2$) and symmetric ν$_s$(CS$_2$) stretching modes, respectively [21–23]. The IR spectra of **I**/**II** also exhibited C–H stretching bands for alkyl substituents at the nitrogen atom of the Dtc ligands [24]: ν$_{as}$(CH$_3$) of 2964/2965 cm^{-1} and ν$_s$(CH$_3$) of 2872/2865 cm^{-1}; ν$_{as}$(CH$_2$) of 2930/2930 cm^{-1} and ν(CH) of 2919 cm^{-1}.

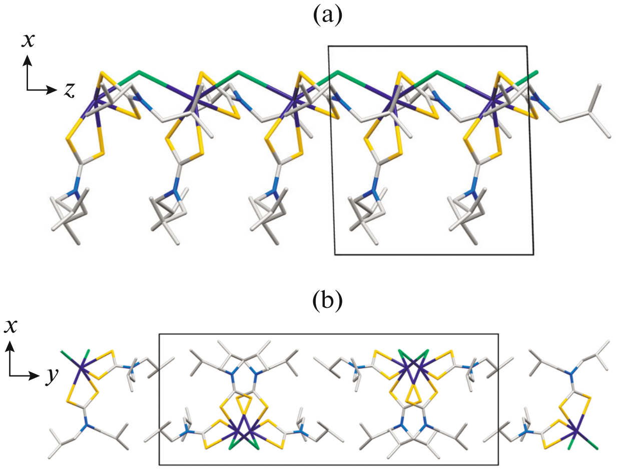

Fig. 2. Projections of the polymer structure of **II** on the (a) *xz* and (b) *xy* planes. The polymer chains are extended along the *z* axis.

The structures of the synthesized bismuth(III) compounds were established by X-ray diffraction. The unit cell of **I**/**II** includes four formula units [Bi{S$_2$CN(C$_3$H$_7$)$_2$}Cl$_2$]/[Bi{S$_2$CN(*iso*-C$_4$H$_9$)$_2$}$_2$Cl] (Table 1, Figs. 1, 2). The inner sphere of the complexes includes one or two Dtc ligands, in which the N–C(S)S bond lengths (1.311–1.332 Å) attest to considerable contribution of double bonding (due to the mesomeric effect of dithiocarbamate groups). As expected from IR spectroscopy data, the N–C(S)S bond length is markedly shorter in complex **I** (1.311 Å) than in complex **II** (1.331 and 1.332 Å).

Similar Bi–S bond lengths (2.6323 and 2.6437 Å) in the former compound (Table 2) dictate a virtually S,S'-isobidentate coordination of the PrDtc ligand. Meanwhile in the latter compound, the coordination mode of the structurally non-equivalent *iso*-BuDtc ligands is clearly S,S'-anisobidentate: the Bi–S bond lengths are 2.6287, 2.7845 Å and 2.6468, 2.7590 Å. The coordination of each dithiocarbamate ligand is accompanied by the formation of the [BiS$_2$C] four-membered metallocycle. In the structure of **I**, the geometry of this ring is nearly perfectly planar: the deviation of the BiSSC and SBiCS torsion angles from 180° does not exceed 0.6° (Table 2). In the structure of **II**, the BiSSC torsion angles (177.7° and 168.8°) attest to different deviations of atoms from the coplanar positions for the two [BiS$_2$C] metallocycles, which may be represented as a small folding between their planes along the S–S axis. The angle between the root-mean-square planes of the rings is close to right angle (85.38(3)°).

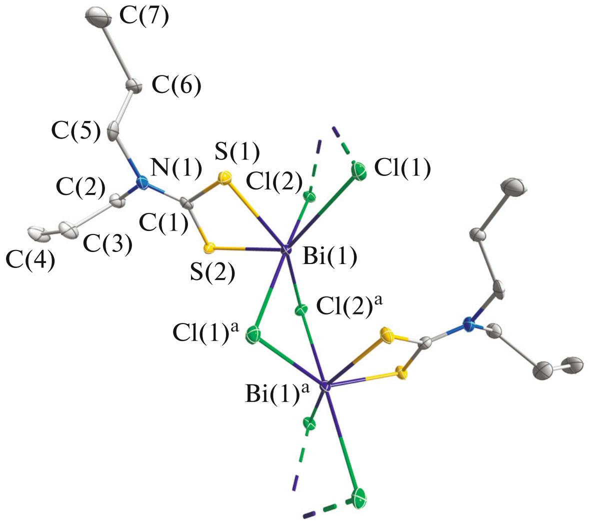

Fig. 3. Two-unit fragment of the $[\mathrm{Bi}\{\mathrm{S_2CN(C_3H_7)_2}\}\mathrm{Cl_2}]_n$ polymer chain. Ellipsoids are drawn at the 50% probability level; symmetry code: ^{a} $1/2 + x$, $1/2 - y$, z. Hydrogen atoms are omitted.

In heteroleptic complexes **I** and **II**, all $\mathrm{Cl^-}$ anions perform μ_2-bridging structural function, which results in asymmetric binding of neighboring $[\mathrm{Bi}\{\mathrm{S_2CN(C_3H_7)_2}\}\mathrm{Cl_2}]$ or $[\mathrm{Bi}\{\mathrm{S_2CN}(iso\text{-}\mathrm{C_4H_9})_2\}_2\mathrm{Cl}]$ molecules, thus forming zigzag-like polymer chains (Figs. 3 and 4) extended along the *x* (**I**) or *z* (**II**) axis.

In both chains, the central atom has a six-coordinate environment, $[\mathrm{BiS_2Cl_4}]$ (in **I**) or $[\mathrm{BiS_4Cl_2}]$ (in **II**) (considering the additional coordination of bridging ligands). The polymer chain in **II** (∠Bi(1)^{a}Bi(1)Bi(1)^b, 156.605(5)°) is somewhat smoother than that in **I** (∠Bi(1)^{a}Bi(1)Bi(1)^b, 148.059(5)°). The significant structural difference between the chains in **I** and **II** is that in the former case, the neighboring metal atoms are bridged by two μ_2-$\mathrm{Cl^-}$ ligands, while in the latter case, only one bridging ligand is involved. Therefore, the coordination unit in **I** is the four-membered metallocycle $[\mathrm{Bi{-}(\mu\text{-}Cl)_2{-}Bi}]$ in the butterfly conformation with a dihedral angle (between the $[\mathrm{BiCl_2}]$ planes) of 140.51(3)°. One Bi–Cl bond length is virtually equal for the two chains (Table 2), whereas other Bi–Cl bond lengths (2.6823–2.8798 Å) are markedly shorter in **I** than in **II** (2.9606 Å). A consequence of the higher binding strength of bismuth atoms in the chain of **I** is the decrease in the Bi–Bi interatomic distance (4.0904(4) Å) compared to this distance in **II** (4.8772(4) Å) or in $[\mathrm{Bi}\{\mathrm{S_2CN(C_3H_7)_2}\}_2\mathrm{Cl}]$ (4.9128(6) Å [4]).

According to heteronuclear (^{13}C, ^{15}N) CP-MAS NMR spectroscopy, crystalline solids **I** and **II** are individual compounds. In the experimental ^{13}C and ^{15}N NMR spectra, the >NC(S)S– groups give rise to one or two (1 : 1) resonance signals (Figs. 5a, 5b), which correctly reflects the presence of one PrDtc ligand or two non-equivalent *iso*-BuDtc ligands in the

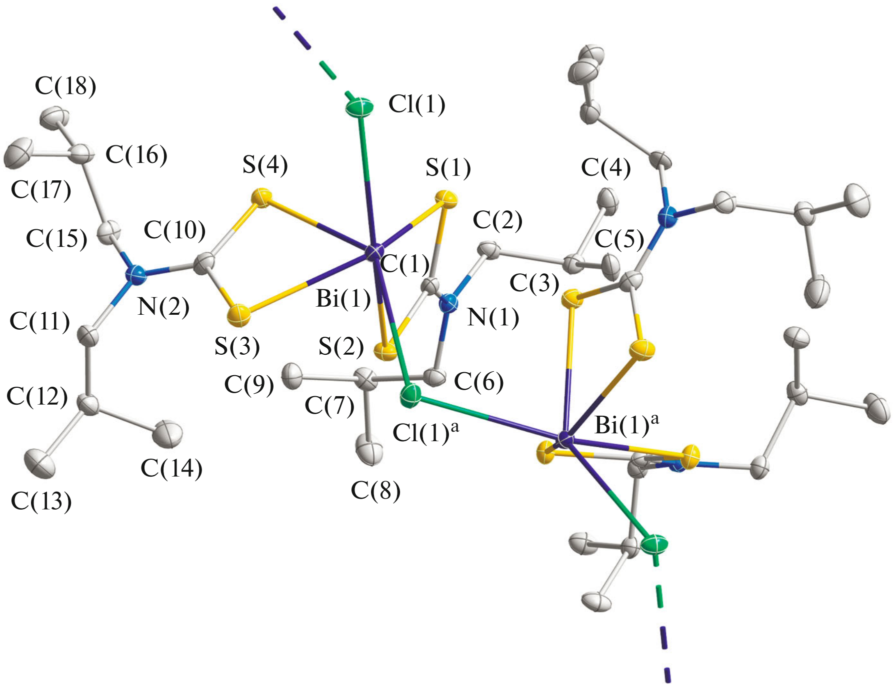

Fig. 4. Two-unit fragment of the $[\mathrm{Bi}\{\mathrm{S_2CN}(iso\text{-}\mathrm{C_4H_9})_2\}_2\mathrm{Cl}]_n$ polymer chain. Ellipsoids are drawn at the 50% probability level; symmetry code: ^{a} x, $3/2 - y$, $-1/2 + z$. Hydrogen atoms are omitted.

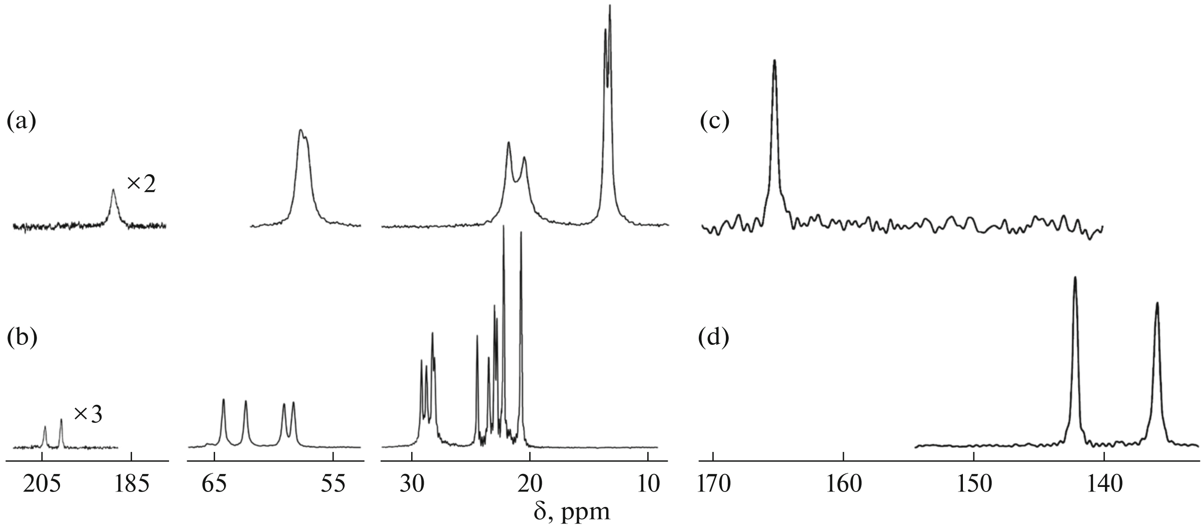

Fig. 5. (a, b) ^{13}C and (c, d) ^{15}N CP-MAS NMR spectra of polycrystalline samples of (a, c) **I** and (b, d) **II**. The number of acquisitions/spinning frequency (Hz) were (a) 2000/5300, (b) 720/6300, (c) 22700/5000, and (d) 85880/4000.

complex. The spectral pattern of >NCH$_2$– (1 : 1), –CH$_2$– (1 : 1), and –CH$_3$ (1 : 1) groups in **I** and >NCH$_2$– (1 : 1 : 1 : 1), >CH– (1 : 1 : 1 : 1), and –CH$_3$ (1 : 1 : 1 : 1 : 2 : 2) groups in **II** attests to non-equivalence of the corresponding chemical groups in the adjacent chains of alkyl substituents, –C$_3$H$_7$ and –*iso*-C$_4$H$_9$, in the dithiocarbamate ligands. It is also noteworthy that the resonance signals of the non-equivalent >NC(S)S– groups in the ^{13}C NMR spectrum of complex **II** show asymmetry, caused by the dipole–dipole coupling of ^{13}C nuclei (I = 1/2) with the ^{14}N quadrupole nucleus (I = 1). The experimental ^{15}N MAS NMR spectra (Figs. 5c, 5d), exhibiting one or two (1 : 1) resonance signals for dithiocarbamate groups, are in full agreement with the ^{13}C NMR data discussed above, thus confirming the presence of the indicated number of PrDtc and *iso*-BuDtc ligands in the crystalline complexes **I** and **II**. A comparison of (^{13}C, ^{15}N) CP-MAS NMR data indicates that transition from the $[Bi\{S_2CN(C_3H_7)_2\}_2Cl]_n$ 1D polymer (the local environment of the central atom is [S$_4$Cl$_2$] [4]) to $[Bi\{S_2CN(C_3H_7)_2\}Cl_2]_n$ (**I**) 1D polymer (the environment is [S$_2$Cl$_4$]) is accompanied by an opposite trend in changes of the ^{13}C and ^{15}N chemical shifts for the >NC(S)S– groups: δ(^{13}C) decrease, on average, by 10.5 ppm, while δ(^{15}N) increase simultaneously by 22.7 ppm. (This fact attests to a higher sensitivity of the ^{15}N chemical shift compared to ^{13}C chemical shift to minor structural differences of dithiocarbamate ligands.)

The thermal behavior of the heteroleptic bismuth(III) complexes was studied by STA with simultaneous recording of the TG and DSC curves under argon (Figs. 6 and 7). Complexes **I**/**II** are thermally stable up to 210/200°C. The corresponding parts of the DSC curves (Figs. 6, *b*, 7, *b*) show endotherms (with peaks at 191.1/138.8°C) caused by melting of complexes: extrapolated $T_{\text{m.p.}}$ = 187.6/132.7°C (melting ranges in a glass capillary: 186–189/131–134°C.) The intense thermolysis of complexes, reflected in steeply declining sections of TG curves, starts at 216/230°C. For complex **II**, it formally occurs in one step (230–305°C) with the main mass loss of 59.76% (Fig. 7, *a*). In the DSC curve, the process of thermolysis is reflected by endotherm at 267.6°C (Fig. 7, *b*). The subsequent smooth section of the TG curve is associated with gradual desorption of the volatile products of thermolysis (1.19%). The mass of the residue (39.05%) formed after completion of the process at 400°C is close to the expected value (calcd. 39.36%) for Bi$_2$S$_3$.

The steeply declining part of the TG curve of compound **I** includes two inflection points at 255 and 317°C, which divide this part into three conjugated steps (Fig. 6, *a*), indicating a complex nature of thermolysis. The mass loss of 19.42% in the first step (210.0–255.0°C) is consistent with the assumption of dissociation of alkyl substituents of the PrDtc ligand (calc. 18.45%). In the second step (255.0–317.0°C) accompanied by a mass loss of 12.19%, the continuing thermolysis of the complex includes dissociation of the Bi–Cl bond (calcd. 15.54%) and reduction of a small portion of bismuth(III) to the elemental state. The latter is indicated by the narrow low-intensity endotherm in the DSC curve at 267.9°C (extrapolated $T_{\text{m.p.}}$ = 267.0°C) caused by melting of bismuth ($T_{\text{m.p.}}$ of the compact metal is 271.442°C [25]). The decrease in the $T_{\text{m.p.}}$ of bismuth is caused by the presence of Bi$_2$S$_3$ as the major component and small size of metal parti-

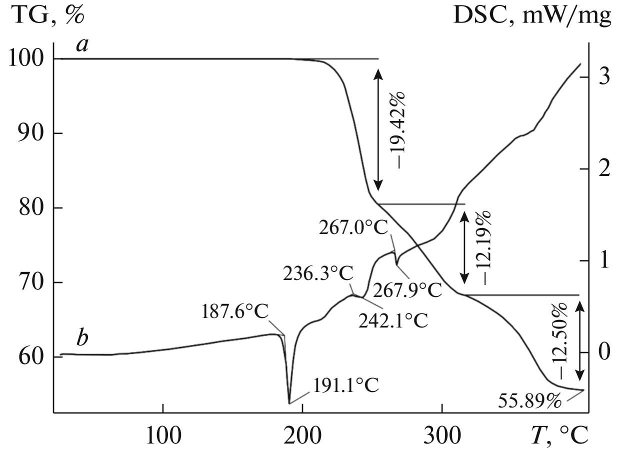

Fig. 6. (*a*) TG and (*b*) DSC curves of complex **I**.

cles [25]. The third step completes the thermolysis to finally give Bi_2S_3 with evaporation of volatile products and stabilization of the mass of the residue (55.89%), which is somewhat lower than that calculated for bismuth(III) sulfide (56.35%).

In both cases, opening of the crucibles revealed black powders, which were investigated by scanning electron microscopy and microprobe analysis. The energy dispersive spectra indicate that the particles of the residue are mainly Bi_2S_3 (Fig. 8a). However, the products of thermolysis were also found to contain reduced bismuth: Fig. 8b shows a spherical particle 70 μm in diameter, which is a hollow microsphere surrounded by Bi_2S_3 particles. In addition, sites of exposure of $BiCl_3$ as thin (~0.15 μm) of thread-like crystals were noted on the sample surface (Fig. 8c).

Thus, new bismuth(III) dithiocarbamato-chlorido complexes $[Bi\{S_2CN(C_3H_7)_2\}Cl_2]$ and $[Bi\{S_2CN(\mathit{iso}\text{-}C_4H_9)_2\}_2Cl]$ were isolated on a preparative scale and characterized in detail by heteronuclear (^{13}C, ^{15}N) CP-MAS NMR spectroscopy, IR spectroscopy, and X-ray diffraction. In the crystalline state, both compounds form zigzag 1D polymer chains involving one or two μ_2-Cl^- ligands, thus completing the environment of the central bismuth atom to sixfold: $[BiS_2Cl_4]$ or $[BiS_4Cl_2]$. The thermal behavior of the heteroleptic bismuth(III) complexes was studied by STA with simultaneous recording of the TG and DSC curves. Study of the residue by microprobe analysis revealed the presence of reduced metallic bismuth and $BiCl_3$ in the samples, apart from Bi_2S_3, formed as the major product of the thermal transformations.

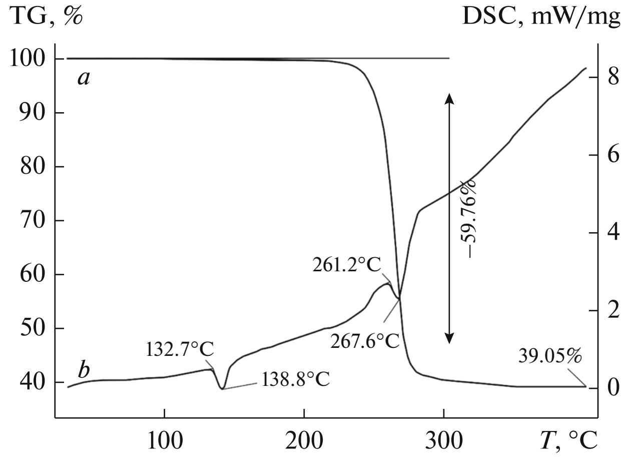

Fig. 7. (*a*) TG and (*b*) DSC curves of complex **II**.

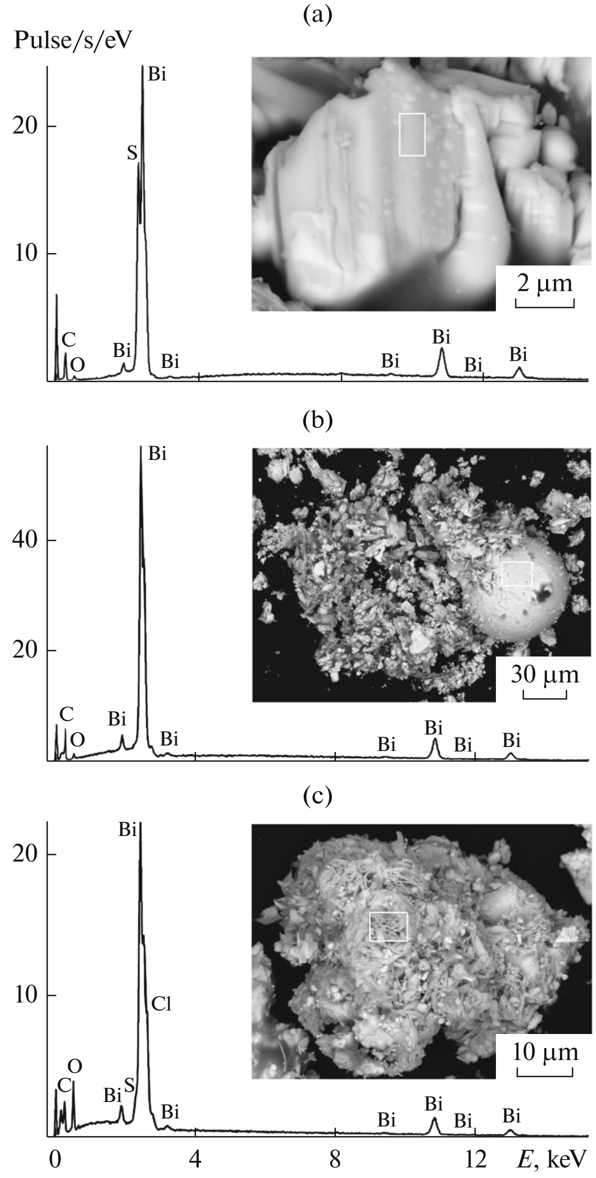

Fig. 8. Particle size and shape and energy dispersive spectra of (a) Bi_2S_3, (b) reduced bismuth, and (c) $BiCl_3$.

ACKNOWLEDGMENTS

X-ray diffraction studies were carried out using research equipment of the Molecular Structure Research Center of the Nesmeyanov Institute of Organoelement Compounds, Russian Academy of Sciences. Electron microscopy studies and recording of energy dispersive spectra were performed at the Analytical Center for Mineralogical and Geochemical Studies of the Institute of Geology and Nature Management, Far Eastern Branch, Russian Academy of Sciences.

The authors are grateful to the Knut and Alice Wallenberg Foundation (NMR for Life program), SciLifeLab Laboratory, and personally to Dr. Tobias Sparrman for help in conducting some ^{13}C CP-MAS NMR experiments at the Umeå University, Umeå, Sweden.

CONFLICT OF INTEREST

The authors declare that they have no conflict of interest.

REFERENCES

1. Koh, Y.W., Lai, C.S., Du, A.Y., et al., *Chem. Mater.*, 2003, vol. 15, no. 24, p. 4544.
2. Ozturk, I.I., Banti, C.N., Kourkoumelis, N., et al., *Polyhedron*, 2014, vol. 67, p. 89.
3. Arda, M., Ozturk, I.I., Banti, C.N., et al., *RSC Adv.*, 2016, vol. 6, no. 35, p. 29026.
4. Novikova, E.V., Ivanov, A.V., Egorova, I.V., et al., *Russ. J. Coord. Chem.*, 2019, vol. 45, no. 10, p. 695. https://doi.org/10.1134/ S1070328419100038
5. Jamaluddin, N.A., Baba, I., Halim, S.N.A., and Tiekink, E.R.T., *Z. Kristallogr. NCS*, 2015, vol. 230, no. 3, p. 239.
6. Battaglia, L.P. and Corradi, A.B., *Dalton Trans.*, 1986, no. 8, p. 1513.
7. Raston, C.L., Rawbottom, G.L., and White, A.H., *Dalton Trans.*, 1981, no. 6, p. 1352.
8. Adeyemi, J.O. and Onwudiwe, D.C., *Molecules*, 2020, vol. 25, no. 2, p. 305.
9. Raston, C.L., Rawbottom, G.L., and White, A.H., *Dalton Trans.*, 1981, no. 6, p. 1366.
10. Raston, C.L., Rawbottom, G.L., and White, A.H., *Dalton Trans.*, 1981, no. 6, p. 1379.
11. Raston, C.L., Rawbottom, G.L., and White, A.H., *Dalton Trans.*, 1981, no. 6, p. 1372.
12. Bharadwaj, P.K., Lee, A.M., Skelton, B.W., et al., *Aust. J. Chem.*, 1994, vol. 47, no. 2, p. 405.
13. Byr'ko, V.M. *Ditiokarbamaty* (Dithiocarbamates), Moscow: Nauka, 1984.
14. Hexem, J.G., Frey, M.H., and Opella, S.J., *J. Chem. Phys.*, 1982, vol. 77, no. 7, p. 3847.
15. Harris, R.K., Jonsen, P., and Packer, K.J., *Magn. Reson. Chem.*, 1985, vol. 23, no. 7, p. 565.
16. Pines, A., Gibby, M.G., and Waugh, J.S., *J. Chem. Phys.*, 1972, vol. 56, no. 4, p. 1776.
17. Ratcliffe, C.I., Ripmeester, J.A., and Tse, J.S., *Chem. Phys. Lett.*, 1983, vol. 99, no. 2, p. 177.
18. Sheldrick, G.M., *Acta Crystallogr., Sect. A: Found. Adv.*, 2015, vol. 71, no. 1, p. 3.
19. Dolomanov, O.V., Bourhis, L.J., Gildea, R.J., et al., *J. Appl. Crystallogr.*, 2009, vol. 42, no. 2, p. 339.
20. Ivanov, A.V., Gerasimenko, A.V., Egorova, I.V., et al., *Russ. J. Coord. Chem.*, 2018, vol. 44, no. 8, p. 518. https://doi.org/10.1134/ S1070328418080043
21. Yin, H.D., Li, F., and Wang, D., *J. Coord. Chem.*, 2007, vol. 60, no. 11, p. 1133.
22. Brown, D.A., Glass, W.K., and Burke, M.A., *Spectrochim. Acta, Part A*, 1976, vol. 32, no. 1, p. 137.
23. Kellner, R., Nikolov, G.S., and Trendafilova, N., *Inorg. Chim. Acta*, 1984, vol. 84, no. 2, p. 233.
24. Kazitsyna, L.A. and Kupletskaya N.B., *Primenenie UF-, IK-, YaMR- i mass-spektroskopii v organicheskoi khimii* (Application of UV, IR, NMR, and Mass Spectroscopy in Organic Chemistry), Moscow: Izd. Mosk. Univ., 1979.
25. Lin, J.-C., Sharma, R.C., and Chang, Y.A., *J. Phase Equilibr.*, 1996, vol. 17, no. 2, p. 132.

Translated by Z. Svitanko